

Combating Enhanced Intracellular Survival (Eis)-Mediated Kanamycin Resistance of *Mycobacterium tuberculosis* by Novel Pyrrolo[1,5-*a*]pyrazine-Based Eis Inhibitors

Atefeh Garzan,[†] Melisa J. Willby,[‡] Huy X. Ngo,[†] Chathurada S. Gajadeera,[†] Keith D. Green,[†] Selina Y. L. Holbrook,[†] Caixia Hou,[†] James E. Posey,^{*,‡} Oleg V. Tsodikov,^{*,†} and Sylvie Garneau-Tsodikova^{*,†} 

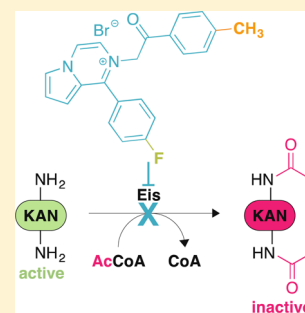
[†]Department of Pharmaceutical Sciences, College of Pharmacy, University of Kentucky, 789 South Limestone Street, Lexington, Kentucky 40536-0596, United States

[‡]Laboratory Branch, Division of Tuberculosis Elimination, National Center for HIV/AIDS, Viral Hepatitis, STD, and TB Prevention, Centers for Disease Control and Prevention, Atlanta, Georgia 30329, United States

Supporting Information

ABSTRACT: Tuberculosis (TB) remains one of the leading causes of mortality worldwide. Hence, the identification of highly effective antitubercular drugs with novel modes of action is crucial. In this paper, we report the discovery and development of pyrrolo[1,5-*a*]pyrazine-based analogues as highly potent inhibitors of the *Mycobacterium tuberculosis* (*Mtb*) acetyltransferase enhanced intracellular survival (Eis), whose up-regulation causes clinically observed resistance to the aminoglycoside (AG) antibiotic kanamycin A (KAN). We performed a structure–activity relationship (SAR) study to optimize these compounds as potent Eis inhibitors both against purified enzyme and in mycobacterial cells. A crystal structure of Eis in complex with one of the most potent inhibitors reveals that the compound is bound to Eis in the AG binding pocket, serving as the structural basis for the SAR. These Eis inhibitors have no observed cytotoxicity to mammalian cells and are promising leads for the development of innovative AG adjuvant therapies against drug-resistant TB.

KEYWORDS: aminoglycoside acetyltransferase, bacterial resistance, enzyme inactivation, drug combination, structure–activity-relationship analysis



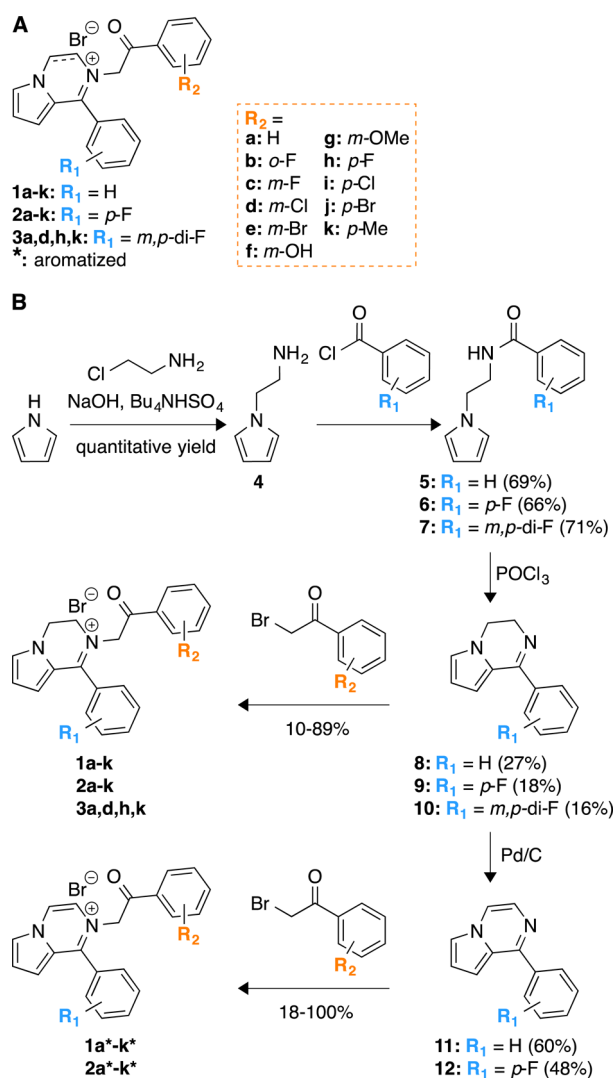
Tuberculosis (TB), caused by the pathogenic *Mycobacterium tuberculosis* (*Mtb*), is the deadliest global bacterial infection. The number of people infected by *Mtb* is currently estimated to be 2–3 billion worldwide.¹ The situation is greatly aggravated by the emergence and spread of difficult or impossible to treat multidrug-resistant (MDR) and extensively drug-resistant (XDR) TB.² Aminoglycoside (AG) antibiotics such as kanamycin A (KAN) and amikacin (AMK) are used for the treatment of MDR and XDR-TB. However, successful outcomes of the treatment of these MDR- and XDR-*Mtb* strains can be impeded as a result of KAN resistance.³ We previously discovered that up-regulation of the enhanced intracellular survival (*eis*) gene, due to point mutations in its promoter, is a cause of resistance to KAN in one-third of KAN-resistant *Mtb* infections in the clinic.^{4,5} The development of new AGs or use of enhanced intracellular survival (Eis) inhibitors are two potential solutions for overcoming the effect of Eis in *Mtb*. We recently demonstrated that Eis is an AG acetyltransferase (AAC) found in a variety of bacterial strains that can inactivate AGs via a multiacetylation mechanism.^{6–11} As Eis has been shown to multiacetylate a wide variety of molecules,^{12,13} including many AG scaffolds, the development of new AGs to combat its action is not likely to be successful. Some metal salts are inhibitory to Eis, but this strategy alone is

not pharmacologically relevant.¹⁴ A better approach would be to use inhibitors of Eis as adjuvant therapies in combination with KAN to combat or forestall the emergence of KAN resistance through Eis up-regulation. We recently reported the discovery and development of Eis inhibitors with an isothiazole *S,S*-dioxide heterocyclic core,¹⁵ and sulfonamide-based,¹⁶ methyl 4*H*-furo[3,2-*b*]pyrrole-5-carboxylate,¹⁷ and 3-(1,3-dioxolano)-2-indolinone¹⁷ scaffolds, which yielded compounds that potentially inhibited Eis in vitro and abolished KAN resistance of the *Mtb* mutant strain K204 that is KAN-resistant due to Eis up-regulation. We previously reported 25 hit compounds identified by high-throughput screening (HTS) of a library composed of ~23,000 small molecules that displayed Eis inhibitory activities.¹⁸ Here, we pursue one of these preliminary hits (compound **1a***, Scheme 1A) and report the chemical synthesis of this compound and that of 47 analogues (Scheme 1B), along with their biochemical and biological studies. Among compounds in this series, we have generated novel and promising Eis inhibitors that not only efficiently inhibit the purified enzyme but also restore KAN sensitivity of KAN-

Received: November 11, 2016

Published: February 13, 2017

Scheme 1. (A) Structures of All Compounds Generated in This Study; (B) Synthetic Scheme Used to Prepare the Compounds in Panel A



resistant *Mtb* bacteria. We also present a crystal structure of Eis in complex with CoA and one potent inhibitor (compound **2k***), which explains the structure–activity relationship (SAR).

Compound **1a*** and 47 additional analogues **1a–3k** with different **R₁** and **R₂** substituents on the two phenyl rings and either a fully aromatized (indicated by an asterisk after the compound number) or a nonaromatized pyrrolo[1,5-*a*]pyrazine core were generated for a thorough SAR analysis of Eis inhibition (Scheme 1B). The synthesis of all compounds started with a reaction between the commercially available pyrrole and 2-chloroethylamine, which afforded compound **4** in quantitative yield. Compound **4** was reacted with different substituted benzoyl chlorides to obtain amides **5–7** in 66–71% yields. The resulting amides were mixed with phosphorus(V) oxychloride to generate cyclized products **8–10**. Then, compounds **8–10** were reacted with various substituted 2-bromoacetophenones to obtain the desired nonaromatized products **1a–k**, **2a–k**, and **3a,d,h,k**. To generate the aromatized counterparts of these products, compounds **8** and **9** were first aromatized in the presence of Pd/C to generate molecules **11** and **12**. Conventionally, Pd/C is a hydrogenation catalyst. In the absence of hydrogen gas, Pd/C is known to catalyze an

oxidative aromatization instead of hydrogenation. More details about this heteroaromatic aromatization were summarized in an excellent review.¹⁹ Compounds **11** and **12** were further reacted with the different substituted 2-bromoacetophenones to furnish the desired fully aromatized analogues **1a*–k*** and **2a*–k***. These compounds were evaluated for Eis inhibition using the clinically relevant KAN as the AG substrate (IC₅₀ values in Table 1).

We first tested whether the freshly synthesized parent compound **1a*** was indeed a potent Eis inhibitor. Expectedly, the freshly synthesized compound **1a*** was found to display potent inhibition of Eis (IC₅₀ = 0.064 ± 0.008 μM), which was ~6-fold better than the IC₅₀ value of the commercially available compound **1a*** (IC₅₀ = 0.36 ± 0.03 μM) from our previous HTS. (Freshly synthesized powders are often more active than HTS library compounds, which may degrade upon storage.¹⁸) The hit scaffold **1a*** contains a pyrrolo[1,5-*a*]pyrazine core, a phenyl ring adjacent to the pyrrolo[1,5-*a*]pyrazine core (containing **R₁**), and an acetophenone moiety (containing **R₂**). A comparison of the chemical structure of compound **1a*** with those of the previously published isothiazole *S,S*-dioxide-based Eis inhibitors cocrystallized with Eis (Figure S160)¹⁵ suggested that **1a*** binds to Eis at the AG binding pocket, similarly to the isothiazole *S,S*-dioxides. Examination of the Eis crystal structure bound to the AG tobramycin (TOB) (PDB: 4JD6²⁰) indicated that the positively charged pyrrolo[1,5-*a*]pyrazine core is presumably essential for binding to the negatively charged AG binding pocket and, thus, should not be modified. On the basis of our previous survey of the hits of this HTS,¹⁸ we also determined that the phenyl ring adjacent to the pyrrolo[1,5-*a*]pyrazine core (containing **R₁**) is likely important for Eis inhibition. In fact, replacing the phenyl ring of **1a*** with an ethyl group resulted in a 25-fold reduction in the inhibitory activity (IC₅₀ = 9.25 ± 1.50 μM).¹⁸ Also, from the crystal structure of Eis in complex with the isothiazole *S,S*-dioxide-based Eis inhibitors, we have rationalized that this phenyl ring is important due to its snug fit in a hydrophobic binding pocket in the AG binding cavity. On the other hand, the π-electron-rich acetophenone moiety (containing **R₂**) and the fully aromatic pyrrolo[1,5-*a*]pyrazine core were predicted to be crucial for binding due to potential π–π interactions with aromatic residues within the Eis binding pocket. However, it remains unexplored whether and which substitutions at **R₁** and **R₂** positions would be beneficial. We hypothesized that (i) tailor fitting the Eis binding pocket by introducing subtle modifications at **R₁** and **R₂** would lead to the discovery of novel optimized inhibitors from our hit scaffold **1a*** and (ii) disruption of the aromaticity of the pyrrolo[1,5-*a*]pyrazine core would be detrimental to the binding affinity of the molecule to the Eis binding pocket. In our biochemical analysis, we will first examine the aromatic compounds and then explore their nonaromatic counterparts. Both the aromatic and nonaromatic molecules are divided into two series. In series 1, **R₁** was kept constant (**R₁** = H), and various substituted acetophenones were installed onto the pyrrolo[1,5-*a*]pyrazine core (changing **R₂**). Similarly, in series 2, **R₁** was kept constant (**R₁** = *p*-F), and the same various substituted acetophenones were installed onto the pyrrolo[1,5-*a*]pyrazine core (changing **R₂**). For the nonaromatic compounds, four additional members were added to a third series (series 3) in which **R₁** was *m,p*-di-F.

We began our analysis of the aromatic compounds by investigating series 1. To probe the ortho position of the acetophenone moiety, compound **1b*** (**R₁** = H, **R₂** = *o*-F) was

Table 1. Inhibition of Eis-Catalyzed KAN Acetylation (IC_{50} Values) by the Pyrrolo [1,5-*a*]pyrazine Derivatives as well as the Effect of These Molecules on KAN MIC Values for *Mtb* H37Rv and KAN-Resistant *Mtb* K204

compd no.	R ₁	R ₂	aromatic	IC_{50}^a (μ M)	H37Rv MIC _{KAN} ^b (μ g/mL)	K204 MIC _{KAN} ^c (μ g/mL)	compd no.	R ₁	R ₂	aromatic	IC_{50}^a (μ M)	H37Rv MIC _{KAN} ^b (μ g/mL)	K204 MIC _{KAN} ^c (μ g/mL)
1a	H	H	no	0.9 ± 0.2	— ^d	—	2a	p-F	H	no	0.47 ± 0.05	—	—
1b	H	o-F	no	0.7 ± 0.2	—	—	2b ^e	p-F	o-F	no	1.4 ± 0.4	—	—
1c	H	m-F	no	0.05 ± 0.01	≤1.25	10, 10	2c	p-F	m-F	no	0.7 ± 0.2	—	—
1d	H	m-Cl	no	0.5 ± 0.1	≤1.25	10, 10	2d	p-F	m-Cl	no	0.15 ± 0.04	≤1.25	>10, >10
1e	H	m-Br	no	0.44 ± 0.16	≤1.25	10, 10	2e	p-F	m-Br	no	0.07 ± 0.02	≤1.25	>10, >10
1f ^e	H	m-OH	no	4.2 ± 1.7	—	—	2f ^e	p-F	m-OH	no	8.7 ± 1.6	—	—
1g	H	m-OMe	no	0.15 ± 0.04	≤1.25	10, 10	2g ^e	p-F	m-OMe	no	1.3 ± 0.4	—	—
1h	H	p-F	no	0.039 ± 0.007	≤1.25	10, 10	2h	p-F	p-F	no	0.23 ± 0.02	≤1.25	10, 5
1i	H	p-Cl	no	0.31 ± 0.09	≤1.25	5, 5	2i	p-F	p-Cl	no	0.5 ± 0.1	—	—
1j	H	p-Br	no	0.76 ± 0.17	—	—	2j ^e	p-F	p-Br	no	1.6 ± 0.5	—	—
1k	H	p-Me	no	0.64 ± 0.18	—	—	2k	p-F	p-Me	no	0.47 ± 0.08	—	—
1a*	H	H	yes	0.064 ± 0.008	≤1.25	5, 5	2a*	p-F	H	yes	0.35 ± 0.07	≤1.25	5, 5
1b*	H	o-F	yes	0.21 ± 0.05	≤1.25	5, 5	2b*	p-F	o-F	yes	0.29 ± 0.07	≤1.25	5, 2.5
1c*	H	m-F	yes	0.06 ± 0.01	≤1.25	5, 5	2c*	p-F	m-F	yes	0.22 ± 0.05	≤1.25	2.5, 2.5
1d*	H	m-Cl	yes	0.025 ± 0.006	≤1.25	5, 5	2d*	p-F	m-Cl	yes	0.06 ± 0.02	≤1.25	5, 5
1e*	H	m-Br	yes	0.34 ± 0.10	≤1.25	2.5, 2.5	2e*	p-F	m-Br	yes	0.06 ± 0.02	≤1.25	5, 5
1f*	H	m-OH	yes	1.8 ± 0.5	≤1.25	10, 5	2f ^{g,e}	p-F	m-OH	yes	8.4 ± 2.8	≤1.25	10, 10
1g*	H	m-OMe	yes	0.21 ± 0.07	≤1.25	5, 5	2g*	p-F	m-OMe	yes	0.53 ± 0.11	≤1.25	5, 2.5
1h*	H	p-F	yes	0.029 ± 0.007	≤1.25	5, 5	2h*	p-F	p-F	yes	0.13 ± 0.04	≤1.25	1.25, 1.25
1i*	H	p-Cl	yes	0.56 ± 0.20	≤1.25	1.25, 1.25	2i*	p-F	p-Cl	yes	0.18 ± 0.06	≤1.25	2.5, 5
1j*	H	p-Br	yes	0.27 ± 0.01	≤1.25	2.5, 2.5	2j*	p-F	p-Br	yes	0.50 ± 0.13	≤1.25	5, 2.5
1k*	H	p-Me	yes	0.19 ± 0.02	≤1.25	2.5, 5	2k*	p-F	p-Me	yes	0.08 ± 0.03	≤1.25	2.5, 5
							3a	m,p-di-F	H	no	0.15 ± 0.05	≤1.25	10, 10
							3d	m,p-di-F	m-Cl	no	0.043 ± 0.006	≤1.25	>10, >10
							3h	m,p-di-F	p-F	no	0.11 ± 0.03	≤1.25	10, 10
							3k	m,p-di-F	p-Me	no	0.11 ± 0.03	≤1.25	10, 10

Control without an Eis inhibitor: 1.25

^a IC_{50} values against purified Eis_ *Mtb* enzyme. ^bAntibacterial activity of KAN against *Mtb* H37Rv. ^cAntibacterial activity of KAN against *Mtb* K204. ^d— indicates that the inhibitor interacted with alamarBlue, resulting in a color change; therefore, it was impossible to determine the MIC using this method. ^eIn MIC assays, the compounds were tested at concentrations that were 100-fold higher than IC_{50} . When the IC_{50} value was >1 μ M, the compounds were not tested at 100 μ M. The compounds were not toxic to *Mtb* in the absence of KAN at these concentrations.

generated and found to display a ~ 3 -fold reduction in Eis inhibitory activity ($IC_{50} = 0.21 \pm 0.05 \mu M$) when compared to the freshly synthesized parent **1a*** (From here on, when comparing to **1a***, we refer to the freshly synthesized **1a***), indicating that ortho substitution was not beneficial. We then explored substitutions at the meta position with compounds **1c***–**1g***. The meta-substituted compound **1c*** ($R_1 = H$, $R_2 = m-F$) was found to have Eis inhibitory activity ($IC_{50} = 0.06 \pm 0.01 \mu M$) comparable to that of the parent compound **1a***. We systematically increased the size of the halogen substituents in compounds **1d*** ($R_1 = H$, $R_2 = m-Cl$) and **1e*** ($R_1 = H$, $R_2 = m-Br$). Interestingly, compound **1d*** displayed an IC_{50} value of $0.025 \pm 0.006 \mu M$, which was ~ 3 -fold smaller than that of the parent compound **1a***. On the other hand, compound **1e*** ($IC_{50} = 0.34 \pm 0.10 \mu M$) was not as potent as compound **1d***, suggesting that the Br substituent was possibly too sterically hindered and, thus, not well tolerated in the Eis binding pocket. Compound **1f*** ($R_1 = H$, $R_2 = m-OH$) ($IC_{50} = 1.8 \pm 0.5 \mu M$) was less potent than the parent compound, which suggested that having a highly polar substituent could be disfavored. Alternatively, replacing the hydroxyl group by a methoxy (compound **1g*** ($R_1 = H$, $R_2 = m-OMe$)) yielded a molecule with improved Eis inhibition ($IC_{50} = 0.21 \pm 0.07 \mu M$) when compared to **1f***. Overall, we found that Cl was the best substituent at the meta position. We pondered whether this trend would translate to the para position, which prompted us to evaluate compounds **1h*** ($R_1 = H$, $R_2 = p-F$), **1i*** ($R_1 = H$, $R_2 = p-Cl$), and **1j*** ($R_1 = H$, $R_2 = p-Br$). Intriguingly, the smaller F substituent was optimal at the para position with an IC_{50} value of $0.029 \pm 0.007 \mu M$, contrary to what we observed at the meta position. Also, inhibitor **1h*** displayed an IC_{50} of $0.029 \pm 0.007 \mu M$, which, similarly to the IC_{50} values for several other inhibitors, was smaller than half of the enzyme concentration used in our assay ($0.25/2 = 0.125 \mu M$). This effect has at least three potential explanations: (1) If inhibition of one monomer per Eis hexamer by one inhibitor molecule leads to the loss of activity of the entire hexamer, then the IC_{50} can, in principle, be as low as $0.125/6 = 0.02 \mu M$. (2) If only a fraction of Eis protein is active in acetylating KAN and binding inhibitors (e.g., due to protein aggregation), then the concentration of active Eis in the assay is an overestimate of the concentration of active enzyme. (3) If inhibitor binding to Eis causes Eis aggregation and inactivates multiple hexamers, then IC_{50} is also a fraction of half of the enzyme concentration in the assay. Mechanism 3 is unlikely, because we do not observe global conformational changes in Eis upon inhibitor binding in crystal structures. Distinguishing among these mechanisms of these highly potent analogues is a goal of ongoing work in our group.

Subsequently, we investigated the effect of R_1 substitutions on the phenyl ring adjacent to the pyrrolo[1,5-*a*]pyrazine core. As the *p*-F substitution was one of the best in terms of activity when we varied R_2 in series **1**, we first decided to install the *p*-F substituent at the R_1 position and generated series **2** analogues. Analogue **2a*** ($R_1 = p-F$, $R_2 = H$) displayed weaker Eis inhibition ($IC_{50} = 0.35 \pm 0.07 \mu M$) than did **1a***. Similarly to **1b*** ($R_1 = H$, $R_2 = o-F$), the ortho-substituted analogue **2b*** ($R_1 = p-F$, $R_2 = o-F$) was also not optimal. When we increased the size of the R_2 substituents at the meta position, we observed that the larger halogens led to more potent Eis inhibition ($Br = Cl > F$) and yielded compounds with IC_{50} values varying from 0.06 to 0.22 μM . Unlike compound **1e*** ($R_1 = H$, $R_2 = m-Br$; $IC_{50} = 0.34 \pm 0.10 \mu M$), the *m*-Br substituted analogue **2e*** ($R_1 = p-F$, $R_2 = m-Br$; $IC_{50} = 0.06 \pm 0.02 \mu M$) was much more

potent, which pointed to the possibility that changing R_1 from H to *p*-F could lead to a slight variation in the binding orientation of the molecule, especially near the meta position of the acetophenone ring. Additionally, the *m*-hydroxy and *m*-methoxy substitutions, as in the cases of **2f*** ($R_1 = p-F$, $R_2 = m-OH$) and **2g*** ($R_1 = p-F$, $R_2 = m-OMe$) either completely abolished Eis inhibitory activity or resulted in moderate inhibition of the enzyme ($IC_{50} = 8.4 \pm 2.8$ and $0.53 \pm 0.11 \mu M$, respectively). This was consistent with the observations made with compounds **1f*** ($R_1 = H$, $R_2 = m-OH$) and **1g*** ($R_1 = H$, $R_2 = m-OMe$). For the para-substituted analogues (**2h*** ($R_1 = p-F$, $R_2 = p-F$), **2i*** ($R_1 = p-F$, $R_2 = p-Cl$), and **2j*** ($R_1 = p-F$, $R_2 = p-Br$)), similarly to what was observed with series **1**, the larger halogen substituents were generally less favorable with activities varying in the range of 0.13–0.50 μM . We also evaluated the para-methylated analogue **2k*** ($R_1 = p-F$, $R_2 = p-Me$) and found that **2k*** displayed excellent activity with an IC_{50} value of $0.08 \pm 0.03 \mu M$, which was 2-fold better than that of **1k*** ($IC_{50} = 0.19 \pm 0.02 \mu M$).

Having established the general SAR trends for the aromatic analogues, we next aimed to determine whether their nonaromatic counterparts (**1a**–**k** and **2a**–**k**) would exhibit decreased activity due to potential disruption of the π – π interactions with Eis aromatic amino acid residues. Indeed, we found that most of the nonaromatic analogues generally displayed less potent Eis inhibition than their aromatic counterparts did. In 4 of 22 cases, the aromatic and nonaromatic compounds displayed nearly equipotent inhibition of Eis. In the case of compounds **1c** and **1c*** ($R_1 = H$, $R_2 = m-F$), the IC_{50} values were virtually the same ($IC_{50} = 0.05 \pm 0.01$ and $0.06 \pm 0.01 \mu M$, respectively). Additionally, compounds **2e** and **2e*** ($R_1 = p-F$, $R_2 = m-Br$) were also practically equipotent in terms of Eis inhibitory activities ($IC_{50} = 0.07 \pm 0.02$ and $0.06 \pm 0.02 \mu M$, respectively). Compounds **1g** and **1g*** ($R_1 = H$, $R_2 = m-OMe$) ($IC_{50} = 0.15 \pm 0.04$ and $0.21 \pm 0.07 \mu M$, respectively) were also similar. For the pair **1i** and **1i*** ($R_1 = H$, $R_2 = p-Cl$) ($IC_{50} = 0.31 \pm 0.09$ and $0.56 \pm 0.20 \mu M$, respectively), the nonaromatic counterpart **1i** was marginally better. Regardless of whether the analogue in series **2** was aromatic or nonaromatic, it was conclusive that at the meta position of the acetophenone moiety, bigger halogen substituents such as Cl and Br were generally better suited, and at the para position of the acetophenone, the smaller F substituent was the best.

Once our pyrrolo[1,5-*a*]pyrazine derivatives were optimized for inhibition of the purified Eis enzyme in vitro, we set out to confirm whether these compounds could display Eis inhibitory activity in the *Mtb* culture by measuring the effect of the compounds on KAN MIC (MIC_{KAN}). Compounds were tested in combination with KAN against the KAN-sensitive H37Rv *Mtb* strain as a control and against the KAN-resistant *Mtb* K204, which is H37Rv *Mtb* bearing a clinically occurring point mutation in the *eis* promoter leading to overexpression of Eis.⁴ *Mtb* H37Rv has an MIC_{KAN} of 1.25 $\mu g/mL$, whereas KAN-resistant *Mtb* K204 has an MIC_{KAN} of $\geq 10 \mu g/mL$. Active compounds were expected to resensitize *Mtb* K204 to KAN. The compounds were generally tested at concentrations that were 100-fold higher than their respective IC_{50} values in the enzymatic assays, to correct for the variation in the potency of Eis inhibition. Weakly potent compounds ($IC_{50} > 1 \mu M$) were tested at 100 μM in the MIC assays. *Mtb* is notorious for its highly lipophilic and complex cell envelope, which provides

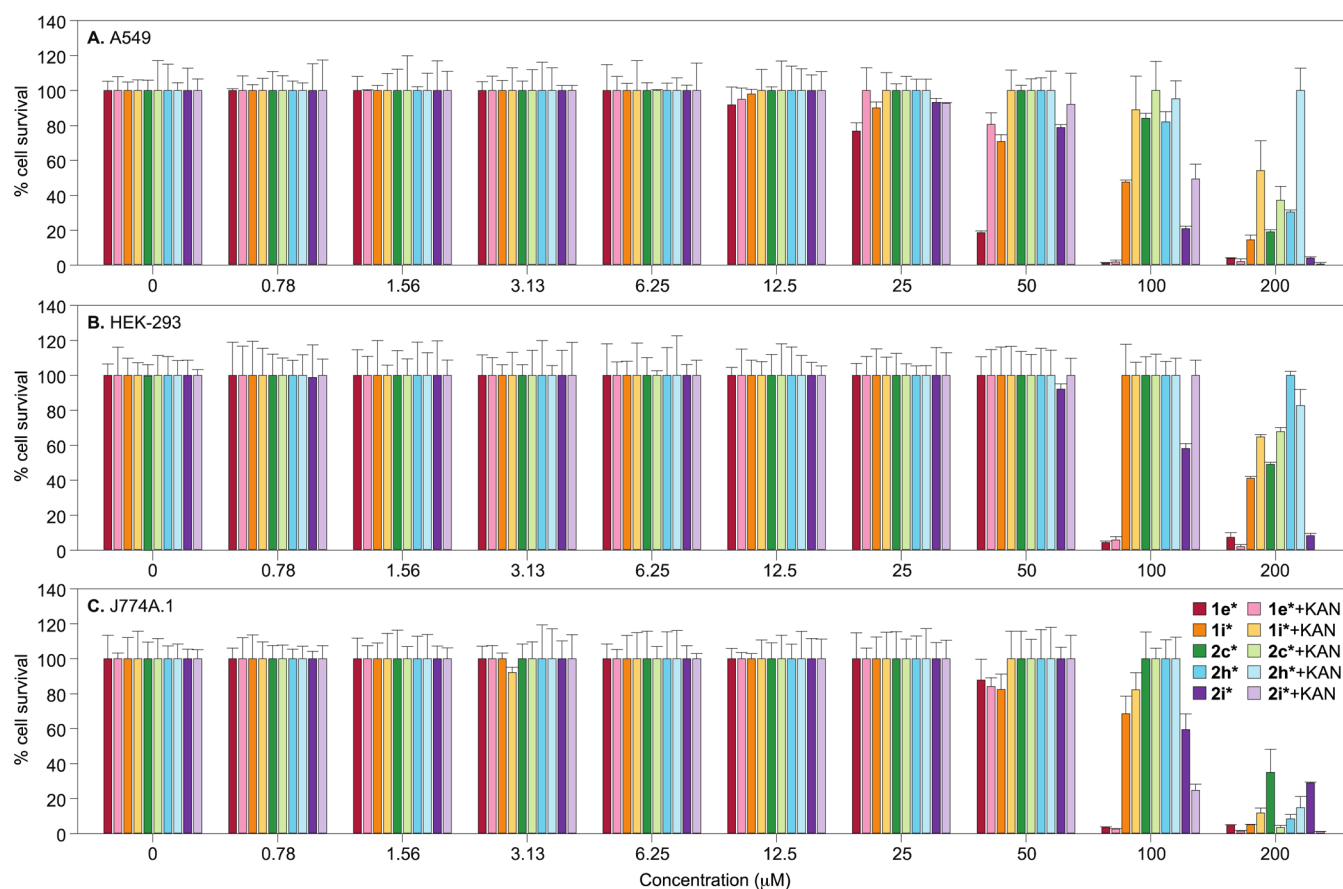


Figure 1. Mammalian cytotoxicity of selected compounds (**1e***, **1i***, **2c***, **2h***, and **2i***) alone (represented as dark color columns) or in the presence of 50 $\mu\text{g}/\text{mL}$ (equivalent to 86 μM) KAN (represented as light color columns immediately to the right of the dark color column of the corresponding compound in the absence of KAN) against (A) A549, (B) HEK-293, and (C) J774A.1 cells. The non-normalized data are presented in [Figure S158](#).

intrinsic resistance to many antibacterial compounds and presents an immense challenge for antitubercular drug discovery. Indeed, as shown in our previous Eis inhibitors studies,¹⁵ some of the most potent in vitro compounds were not active in *Mtb* cultures. We also cannot exclude low solubility or aggregation of the compounds in the culture media as a reason for poor activity. Herein, we determined the MIC values for KAN (MIC_{KAN}) against *Mtb* K204 in the absence or presence of our Eis inhibitors and compared them to the MIC_{KAN} of the drug-sensitive *Mtb* H37Rv strain. As anticipated, most compounds caused a reduction in the MIC_{KAN} for *Mtb* K204, overcoming KAN resistance. Poor Eis inhibitors such as compounds **1f*** and **2f*** with relatively high IC_{50} values were unable to resensitize *Mtb* K204 to the action of KAN. These observations, together with the lack of toxicity of these inhibitors when used without KAN for either *Mtb* strains, validate Eis inhibition as the principal mechanism of MIC_{KAN} reduction by these compounds. *Mtb* H37Rv, for which MIC_{KAN} is virtually unaffected by the inhibitors, serves as an important negative control in this regard. Some of the good Eis inhibitors, such as compounds **1c**–**1e**, **1g**, **1h**, **2d**, **2e**, **2h**, **3a**, **3d**, **3h**, and **3k**, did not resensitize *Mtb* K204 to the action of KAN despite their nanomolar IC_{50} values ($\text{MIC}_{\text{KAN}} \geq 10 \mu\text{g}/\text{mL}$), indicating that these molecules may not go through the cell envelope. Compounds **1a***–**1e***, **1g***, **1h***, **1i**, **1j***, **1k***, **2a***–**2e***, **2g***, and **2i***–**2k*** partially restored the activity of KAN ($\text{MIC}_{\text{KAN}} = 2.5$ – $5 \mu\text{g}/\text{mL}$). Generally, the analogues in series 1 and 2

displayed better potency compared to the analogues in series 3 in *Mtb* culture. Although the charged nature of these compounds may contribute adversely to the permeability of the compounds through the greasy mycobacterial cell envelope, their better solubility in aqueous solution when compared to other uncharged Eis inhibitors may offset this potential issue. Therefore, these compounds serve as valuable alternatives to our previously reported uncharged Eis inhibitors of other scaffolds in further preclinical development of Eis inhibitors as KAN adjuvants in TB therapy. Indeed, two compounds, **1i*** and **2h***, are highly promising for future development, as they completely restore the potency of KAN, fully overcoming Eis up-regulation.

Cytotoxicity to three different mammalian cell lines was tested for five representative potent Eis inhibitors ([Figure 1](#)) in the absence and presence of KAN at the concentration of 50 $\mu\text{g}/\text{mL}$ (equivalent to 86 μM), greatly exceeding the MIC_{KAN} of *Mtb*. The negative control corresponded to no inhibitor treatment and was standardized as 100% cell survival. The positive control was a treatment with Triton X-100, where we observed most of the cells killed. The normalized and non-normalized cytotoxicity data are presented in [Figure 1](#) and [Figure S158](#), respectively. We observed that at sub- IC_{50} concentrations, our Eis inhibitors induced cell proliferation, thereby displaying >100% cell survival. With the exception of compound **1e***, which at 50 μM exhibited significant cytotoxicity against one of the three cell lines, none of the

compounds were cytotoxic against any of the three cell lines up to 50 μM . Three compounds (**1i***, **2c***, and **2h***) had no significant cytotoxicity up to 100 μM , without or with KAN. The lack of cytotoxicity indicates the absence of toxic off-target effects in the mammalian cells, strengthening the promise of these compounds as candidates for animal and clinical studies. Eis inhibitors appear to be less toxic when they are co-administered with KAN. Upon assessing the cytotoxicity of KAN alone (Figure S159) and Eis inhibitors alone (Figure 1 and Figure S158), one can observe that exposure to KAN or to Eis inhibitors alone at sub- IC_{50} concentrations promotes cell growth. This phenomenon of increased growth in the presence of small quantities of xenobiotics has been previously observed.^{21–25} Due to this effect, cotreatment with KAN and Eis inhibitors may result in a faster cell growth than that for KAN alone.

To rationalize our SAR study and understand the binding mode of our inhibitors to Eis, we determined a crystal structure of Eis in complex with CoA and inhibitor **2k*** (one of our best inhibitors; $\text{IC}_{50} = 0.08 \pm 0.03 \mu\text{M}$) at the resolution of 2.4 Å (Figure 2 and Table S1). The crystal structure demonstrates that inhibitor **2k*** is indeed bound in the AG binding site (established by our reported Eis-CoA-TOB crystal structure;²⁰ Figure S160) and is stabilized in the bound state by numerous hydrophobic interactions with Eis. The pyrazine ring is stacked between the side chain of Glu401 of Eis and its C-terminal carboxyl group, with mutually orthogonal π – π interactions of the pyrazine ring with the indole ring of Trp36. This observation supports our initial hypothesis that the aromaticity of the pyrrolo[1,5-*a*]pyrazine core is crucial for activity and explains why aromatized compounds resulted in better activities during SAR analysis. Attached to the pyrrolo[1,5-*a*]pyrazine core, the acetophenone ring displayed parallel π – π interaction with Phe84 and showed that our prediction about the importance of the aromatic acetophenone was correct. Additionally, the R_2 -substituted acetophenone fits in a mainly hydrophobic environment of Leu63, Trp36, and Arg37. Hence, adding a polar hydroxyl group at R_2 , such as in compounds **1f**, **1f***, **2f**, and **2f***, destabilizes binding within the hydrophobic environment and results in weaker Eis inhibitory activity. Furthermore, the para position of the acetophenone ring is sterically restrained on all sides, being sandwiched between Phe84 and Trp36 as well as abutting Trp13 and Met65, explaining why the larger groups in para position, such as in compounds **1i/i***, **1j/j***, **2i/i***, and **2j/j***, resulted in decreased Eis inhibitory activities. This R_2 binding pocket of Eis accommodates structurally similar substitutions to that of our previously published inhibitors with different core scaffolds (Figure S160). Otherwise, these previously reported inhibitors are bound in distinct orientations in the large AG binding cavity. As shown in Figure 2 and in our SAR analysis, near the two meta positions of the acetophenone ring, there are spacious pockets allowing incorporation of larger substituents at the meta position without compromising activity. Finally, the phenyl ring containing R_1 is located in a spacious binding pocket lined by the terminus of the phosphopantetheinyl tail of the CoA molecule, Asp26, the C-terminal carboxyl group, Ser83, and Phe24, explaining why a phenyl group is preferred over an ethyl group at the R_1 position. In summary, the crystal structure of the EisC204A-CoA-inhibitor **2k*** complex allowed us to explain our biological data and provides a basis for future additional structure-based development of Eis inhibitors.

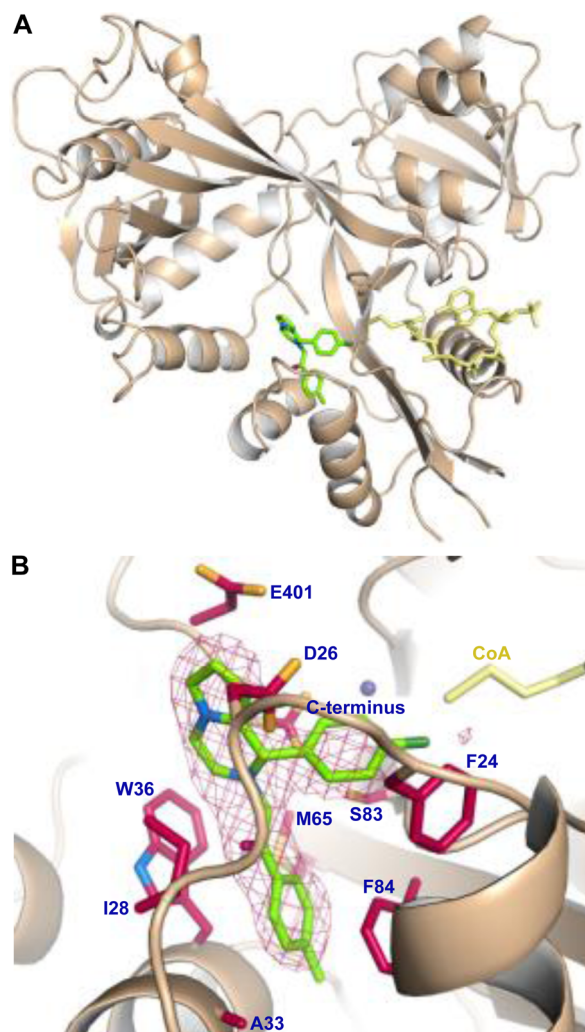


Figure 2. (A) Crystal structure of EisC204A-CoA-inhibitor **2k*** complex (PDB ID 5TVJ). CoA is colored yellow. Compound **2k*** is colored green. (B) Zoom-in view of the binding pocket of compound **2k***. Amino acid residues that are interactive with compound **2k*** are highlighted in red. The strong omit $F_o - F_c$ electron density map contoured at 3σ generated without the inhibitor is shown by the mesh, demonstrating that the inhibitor molecule is unambiguously defined by the X-ray diffraction data.

In conclusion, via a SAR study, we tailor-fitted Eis inhibitors possessing the pyrrolo[1,5-*a*]pyrazine core to its Eis binding pocket and identified multiple novel nanomolar potency inhibitors. We validated our hypothesis that the aromaticity of the pyrrolo[1,5-*a*]pyrazine core was important for activity and that aromatic analogues were overall better inhibitors than their nonaromatic counterparts. For the aromatic analogues, our study indicated that the SAR strongly correlates with the size of the halogen substituent(s). At the meta position of the acetophenone, bigger halogens such as Cl and Br were generally well tolerated. On the other hand, at the para position, substitutions of a smaller F atom and a methyl group produced analogues with substantially improved activities. The SAR analysis also revealed that the substitution of a polar functional group such as the hydroxyl group greatly perturbed the hydrophobic environment, leading to decreased activity. These SAR observations were explained by the crystal structure analysis, which will greatly facilitate future medicinal chemistry studies. Most significantly, by in vitro *Mtb* culture assays, we

confirmed that our Eis inhibitors were capable of penetrating the *Mtb* cell wall and canceling the KAN resistance of *Mtb* K204, which overexpresses Eis. As exemplified by a clinically used combination of a β -lactamase inhibitor, clavulanic acid, and penicillin, these Eis inhibitors may become similarly significant as adjuvant molecules in a combination therapy with KAN to prevent the emergence of and combat KAN resistance in MDR- and XDR-TB.

■ ASSOCIATED CONTENT

● Supporting Information

The Supporting Information is available free of charge on the ACS Publications website at DOI: 10.1021/acsinfecdis.6b00193.

All experimental procedures and characterization data of all new compounds synthesized as well as their ^1H and ^{13}C NMR spectra and HPLC traces (Figures S1–S156). Representative IC_{50} curves (Figure S157). Plots showing the non-normalized cytotoxicity data (the normalized data in Figure 1) are provided in Figure S158. Plots showing that KAN alone is not toxic to three mammalian cell lines in the concentration range tested (Figure S159). Finally, superimposition of the crystal structure of Eis in complex with inhibitors and TOB (Figure S160). A table of X-ray diffraction data collection and refinement statistics for the EisC204A-CoA-inhibitor 2k^* complex (Table S1) is also provided (PDF)

■ AUTHOR INFORMATION

Corresponding Authors

*(S.G.-T.) E-mail: sylviegttsodikova@uky.edu. Phone: (859) 218-1686. Fax: (859) 257-7585.

*(J.E.P.) E-mail: jposey@cdc.gov.

*(O.V.T.) E-mail: oleg.tsodikov@uky.edu.

ORCID

Sylvie Garneau-Tsodikova: 0000-0002-7961-5555

Author Contributions

The manuscript was written through contributions of all authors. All authors have given approval to the final version of the manuscript.

Funding

This study was funded by a National Institutes of Health (NIH) Grant AI090048 (S.G.-T.), a grant from the Firland Foundation (S.G.-T.), a grant from the Center for Chemical Genomics (CCG) at the University of Michigan (S.G.-T.), and startup funds from the College of Pharmacy at the University of Kentucky (S.G.-T. and O.V.T.). S.Y.L.H. is partially supported by a University of Kentucky Presidential Fellowship.

Notes

Use of trade names is for identification only and does not constitute endorsement by the U.S. Department of Health and Human Services, the U.S. Public Health Service, or the CDC. The findings and conclusions expressed by the authors do not necessarily reflect the official opinion of the Centers for Disease Control and Prevention or the authors' affiliated institutions. The authors declare no competing financial interest.

■ ACKNOWLEDGMENTS

We thank Martha Larsen, Steve Vander Roest, and Paul Kirchhoff (from the CCG) for their help with HTS.

■ ABBREVIATIONS

AAC, aminoglycoside *N*-acetyltransferase; AG, aminoglycoside; AMK, amikacin; CoA, coenzyme A; Eis, enhanced intracellular survival; HTS, high-throughput screening; KAN, kanamycin A; MDR, multidrug-resistant; MIC, minimum inhibitory concentration; *Mtb*, *Mycobacterium tuberculosis*; SAR, structure–activity relationship; TB, tuberculosis; TOB, tobramycin; XDR, extensively drug-resistant

■ REFERENCES

- (1) World Health Organization. (2016) *Global Tuberculosis Report*; Geneva, Switzerland.
- (2) Gandhi, N. R., Nunn, P., Dheda, K., Schaaf, H. S., Zignol, M., van Soolingen, D., Jensen, P., and Bayona, J. (2010) Multidrug-resistant and extensively drug-resistant tuberculosis: a threat to global control of tuberculosis. *Lancet* 375, 1830–1843.
- (3) Yew, W. W., Lange, C., and Leung, C. C. (2011) Treatment of tuberculosis: update 2010. *Eur. Respir. J.* 37, 441–462.
- (4) Zaunbrecher, M. A., Sikes, R. D., Jr., Metchock, B., Shinnick, T. M., and Posey, J. E. (2009) Overexpression of the chromosomally encoded aminoglycoside acetyltransferase eis confers kanamycin resistance in *Mycobacterium tuberculosis*. *Proc. Natl. Acad. Sci. U. S. A.* 106, 20004–20009.
- (5) Campbell, P. J., Morlock, G. P., Sikes, R. D., Dalton, T. L., Metchock, B., Starks, A. M., Hooks, D. P., Cowan, L. S., Plikaytis, B. B., and Posey, J. E. (2011) Molecular detection of mutations associated with first- and second-line drug resistance compared with conventional drug susceptibility testing of *Mycobacterium tuberculosis*. *Antimicrob. Agents Chemother.* 55, 2032–2041.
- (6) Chen, W., Biswas, T., Porter, V. R., Tsodikov, O. V., and Garneau-Tsodikova, S. (2011) Unusual regioversatility of acetyltransferase Eis, a cause of drug resistance in XDR-TB. *Proc. Natl. Acad. Sci. U. S. A.* 108, 9804–9808.
- (7) Tsodikov, O. V., Green, K. D., and Garneau-Tsodikova, S. (2014) A random sequential mechanism of aminoglycoside acetylation by *Mycobacterium tuberculosis* Eis protein. *PLoS One* 9, e92370.
- (8) Green, K. D., Pricer, R. E., Stewart, M. N., and Garneau-Tsodikova, S. (2015) Comparative study of Eis-like enzymes from pathogenic and non-pathogenic bacteria. *ACS Infect. Dis.* 1, 272–283.
- (9) Chen, W., Green, K. D., Tsodikov, O. V., and Garneau-Tsodikova, S. (2012) Aminoglycoside multiacetylating activity of the enhanced intracellular survival protein from *Mycobacterium smegmatis* and its inhibition. *Biochemistry* 51, 4959–4967.
- (10) Green, K. D., Biswas, T., Chang, C., Wu, R., Chen, W., Janes, B. K., Chalupska, D., Gornicki, P., Hanna, P. C., Tsodikov, O. V., Joachimiak, A., and Garneau-Tsodikova, S. (2015) Biochemical and structural analysis of an Eis family aminoglycoside acetyltransferase from *Bacillus anthracis*. *Biochemistry* 54, 3197–3206.
- (11) Pricer, R. E., Houghton, J. L., Green, K. D., Mayhoub, A. S., and Garneau-Tsodikova, S. (2012) Biochemical and structural analysis of aminoglycoside acetyltransferase Eis from *Anabaena variabilis*. *Mol. Biosyst.* 8, 3305–3313.
- (12) Houghton, J. L., Green, K. D., Pricer, R. E., Mayhoub, A. S., and Garneau-Tsodikova, S. (2013) Unexpected *N*-acetylation of capreomycin by mycobacterial Eis enzymes. *J. Antimicrob. Chemother.* 68, 800–805.
- (13) Kim, K. H., An, D. R., Song, J., Yoon, J. Y., Kim, H. S., Yoon, H. J., Im, H. N., Kim, J., Kim, D. J., Lee, S. J., Kim, K. H., Lee, H. M., Kim, H. J., Jo, E. K., Lee, J. Y., and Suh, S. W. (2012) *Mycobacterium tuberculosis* Eis protein initiates suppression of host immune responses by acetylation of DUSP16/MKP-7. *Proc. Natl. Acad. Sci. U. S. A.* 109, 7729–7734.
- (14) Li, Y., Green, K. D., Johnson, B. R., and Garneau-Tsodikova, S. (2015) Inhibition of aminoglycoside acetyltransferase resistance enzymes by metal salts. *Antimicrob. Agents Chemother.* 59, 4148–4156.
- (15) Willby, M. J., Green, K. D., Gajadeera, C. S., Hou, C., Tsodikov, O. V., Posey, J. E., and Garneau-Tsodikova, S. (2016) Potent inhibitors

of acetyltransferase Eis overcome kanamycin resistance in *Mycobacterium tuberculosis*. *ACS Chem. Biol.* 11, 1639–1646.

(16) Garzan, A., Willby, M. J., Green, K. D., Gajadeera, C. S., Hou, C., Tsodikov, O. V., Posey, J. E., and Garneau-Tsodikova, S. (2016) Sulfonamide-based inhibitors of aminoglycoside acetyltransferase Eis abolish resistance to kanamycin in *Mycobacterium tuberculosis*. *J. Med. Chem.* 59, 10619–10628.

(17) Garzan, A., Willby, M. J., Green, K. D., Tsodikov, O. V., Posey, J. E., and Garneau-Tsodikova, S. (2016) Discovery and optimization of two Eis inhibitor families as kanamycin adjuvants against drug-resistant *M. tuberculosis*. *ACS Med. Chem. Lett.* 7, 1219.

(18) Green, K. D., Chen, W., and Garneau-Tsodikova, S. (2012) Identification and characterization of inhibitors of the aminoglycoside resistance acetyltransferase Eis from *Mycobacterium tuberculosis*. *ChemMedChem* 7, 73–77.

(19) Kawashita, Y., and Hayashi, M. (2009) Synthesis of heteroaromatic compounds by oxidative aromatization using an activated carbon/molecular oxygen system. *Molecules* 14, 3073–3093.

(20) Houghton, J. L., Biswas, T., Chen, W., Tsodikov, O. V., and Garneau-Tsodikova, S. (2013) Chemical and structural insights into the regioversatility of the aminoglycoside acetyltransferase Eis. *ChemBioChem* 14, 2127–2135.

(21) Quave, C. L., Estevez-Carmona, M., Compadre, C. M., Hobby, G., Hendrickson, H., Beenken, K. E., and Smeltzer, M. S. (2012) Ellagic acid derivatives from *Rubus ulmifolius* inhibit *Staphylococcus aureus* biofilm formation and improve response to antibiotics. *PLoS One* 7, e28737.

(22) Hall, B. S., Bot, C., and Wilkinson, S. R. (2011) Nifurtimox activation by trypanosomal type I nitroreductases generates cytotoxic nitrile metabolites. *J. Biol. Chem.* 286, 13088–13095.

(23) Xu, W., Zhu, X., Tan, T., Li, W., and Shan, A. (2014) Design of embedded-hybrid antimicrobial peptides with enhanced cell selectivity and anti-biofilm activity. *PLoS One* 9, e98935.

(24) Shrestha, S. K., Fosso, M. Y., Green, K. D., and Garneau-Tsodikova, S. (2015) Amphiphilic tobramycin analogues as antibacterial and antifungal agents. *Antimicrob. Agents Chemother.* 59, 4861–4869.

(25) Fosso, M. Y., Shrestha, S. K., Green, K. D., and Garneau-Tsodikova, S. (2015) Synthesis and bioactivities of kanamycin B-derived cationic amphiphiles. *J. Med. Chem.* 58, 9124–9132.